

**THE DEVELOPMENT OF VERY HIGH STRENGTH COPPER ALLOYS WITH
RESISTANCE TO HYDROGEN EMBRITTLEMENT AND STRESS CORROSION
CRACKING**

Clive D S Tuck
Langley Alloys, Meighs Ltd,
Stoke-on-Trent, UK

SUMMARY

Several types of very high strength copper nickel alloys are tested with respect to environment sensitive mechanical properties which include hydrogen embrittlement and exposure to sulfide and ammonium compounds. It is found that Cu-Ni-Al-Mn-Nb alloys with nickel content up to 25wt% are resistant to hydrogen embrittlement, sulfide stress corrosion and stress corrosion in ammonium environments, whereas Cu-Ni-Sn materials demonstrate susceptibility to stress corrosion. A study of factors controlling stress corrosion susceptibility of Cu-Ni-Al and Cu-Ni-Al-Mn-Nb alloys shows the principal influences to be the degree of age hardening, the grain size and the iron content. Thus it is found necessary to control the production process of very high strength Cu-Ni-Al-Mn-Nb alloys such that high mechanical strengths are achieved with the material's possessing a fine grain size and being in an under-aged condition. The use of the NACE TM-01-98-98 slow strain rate tensile test is advocated as a production test method for very high strength copper alloys to verify resistance to stress corrosion cracking susceptibility.

Keywords: Copper-nickel, stress corrosion, hydrogen embrittlement, ammonia, amines, ammoniacal, high strength, slow strain rate test, precipitation hardening.

INTRODUCTION

Copper-nickel alloys have had a long history of use in marine environments due to their high corrosion resistance and good anti-fouling properties. ¹ As a means of improving the mechanical strength of these type of alloys, two principal alloying methods have been reported in the literature; one of which involves the addition of aluminium ² and the other, the addition of tin. ³ Aluminium addition increases strength by a conventional precipitation hardening mechanism, whereas Cu-Ni-Sn alloys display spinodal strengthening through the development of submicroscopic chemical composition fluctuations. ⁴ In the case of Cu-Ni-Al, the principal hardening precipitate has been found to be Ni₃Al (γ'), ⁵ which is the same type of precipitate as is commonly found in nickel superalloys. Both alloy types are able to achieve high strengths, matching that of carbon steel,

although the Cu-Ni-Al type alloys are generally able to produce higher ductility and have therefore been found to be more useful for engineering purposes. Additional elements have been introduced to the basic Cu-Ni-Al ternary alloy in order to produce alloys which are able to be manufactured to achieve properties which optimize strength and ductility. It has been found⁶ that the Ni₃Al precipitation occurs much more effectively after hot-working due to the density of nucleation sites available. Also, the addition of iron increases the hardening effectiveness of Ni₃Al and niobium additions cause an increased volume of Ni₃Al to precipitate out.^{6, 7} Development work to optimise the chemical composition, thermo-mechanical processing and cooling after hot working has produced the high strength Cu-Ni-Mn-Al-Nb alloy, MARINEL⁽¹⁾ 220. This material is able to offer a 0.2% proof stress of over 700 N/mm² together with a ductility over 15% for section thicknesses up to 100 mm as well as resistance to hydrogen embrittlement and stress corrosion cracking. The alloy has been widely used for offshore engineering in applications which have included high strength fasteners, high integrity connectors and the wide variety of actuator devices.

Raising the strength of copper-nickel alloys could have the adverse effect of increasing the possibility of environment-sensitive mechanical behavior, and this paper gives details of hydrogen embrittlement and stress corrosion tests which have been carried out on the very high strength copper-nickels Cu-Ni-Sn, Cu-Ni-Al and Cu-Ni-Al-Mn-Nb. For the Cu-Ni-Al(-Mn-Nb) alloys, an investigation into the factors which can influence their behaviour in debilitating environments is reported, linking this with previous work which has been carried out on the metallurgy⁷ and stress corrosion behavior^{8,9} of these materials. Finally, the ways in which this information has been used to develop improved products is presented.

EXPERIMENTAL PROCEDURE

Materials Tested

The materials tested were produced as bar products in the diameter range 25-35mm. The types of alloys used were Cu-Ni-Sn (UNS C72900), Cu-Ni-Al (W Nr 2.1504) and Cu-Ni-Al-Mn-Nb (UNS C72420-type). The compositions and mechanical properties of these are given in Table 1 and Table 2.

Hydrogen Embrittlement Testing

Testing to determine the hydrogen embrittlement resistance of the high strength Cu-Ni-Al-Mn-Nb alloys was carried out by slow strain rate stress testing under conditions of hydrogen charging. Before testing, the tensile test piece was immersed in synthetic seawater (SSW) at 24°C for a period of 24h with polarization to -1050mV vs SCE. The SSW was aerated by continuously bubbling air through the medium. The alloys used were MAR216, MAR217, MAR218 and MAR219, representing a nickel range of 19% to 25%. During the test, the specimens were polarised at -1000 mV vs SCE and the strain rate used was $2 \times 10^{-6} \text{ s}^{-1}$. Ductility ratios were established between each specimen stressed to failure under hydrogen charging conditions and another specimen tested in air. Also, after each test, the fractured specimen was observed under a 20x magnification to determine the mode of failure.

Comparative stress corrosion resistance of different high strength copper-nickels

Standard stress corrosion test methods were employed to compare the different alloys. These were the NACE TM-01-77 sulfide stress corrosion test and NACE TM-01-98-98 slow strain rate test. The TM-01-77 tests were carried out at ambient temperature with the specimens statically loaded at their 0.2% Proof Stress for 720 hours. The environment used was of 500 cm³ volume consisting of 50 g/l sodium chloride with 5 g/l acetic through which passed a few bubbles per minute of hydrogen sulfide. Initial deaeration was achieved by using oxygen-free nitrogen at 200 cm³ per minute for 1 hour plus a further 30 minutes in the test cell, followed by H₂S

⁽¹⁾ MARINEL[®] is a registered Trademark of Langley Alloys, Meighs Ltd

saturation at 200 cm³/min for 30 minutes. Alloy samples used were MTA150 (Cu-Ni-Sn) and the Cu-Ni-Al-Mn-Nb alloys MAR216, MAR217, MAR218 and MAR219.

Slow strain rate testing was carried out at a strain rate of 10⁻⁵ s⁻¹. Tensile specimens had a gauge length of 30.0 mm and a gauge diameter of 3.50 mm (± 0.05 mm) with a gauge surface finish of 5 µm. The environment used in this series of tests was 10% ammonium chloride at 82°C. Materials used were MTA150 (Cu-Ni-Sn), HMA120 (Cu-Ni-Al) and MAR220 (Cu-Ni-Al-Mn-Nb). Ratios of ductility and fracture face reduction in area were determined using values obtained from tests carried out in the environment compared to the values obtained from a similar test in air. After each slow strain rate test, the fracture surface and surrounding necked gauge length was examined on a x40 optical microscope in order to determine the visual degree of ductility of the fracture.

Investigation of the factors controlling stress corrosion susceptibility of Cu-Ni-Al and Cu-Ni-Al-Mn-Nb alloys.

Degree of Aging - Heat treatment in the range 400°C-600°C. An investigation was carried out to determine the effect of aging of Cu-Ni-Al-Mn-Nb alloys in the temperature range 400°C-500°C on stress corrosion susceptibility.¹⁰ In order to determine whether there is a relationship between the degree of ageing and stress corrosion susceptibility of Cu-Ni-Al-Mn-Nb, samples of as-rolled MAR208 were taken and heat treated for 2.5 h, 5 h and 10 h. Slow strain rate tensile tests were then carried out in 10% sodium chloride at 80°C using a strain rate of 1.25 x 10⁻⁶ s⁻¹.

Grain Growth and Solutionizing/ Heat treatment above 850°C. An investigation was undertaken to establish whether stress corrosion susceptibility of Cu-Ni-Al-Mn-Nb alloys could be induced by heat treatment at temperatures above 850°C, which would produce grain growth and would cause Ni₃Al precipitates to go into solution, allowing the precipitate to reform during air cooling. A sample of as-rolled MAR209 was heat treated at 1000°C for 2 h followed by cooling in air to 600°C and holding at 600°C for 2 h before a final air cool. The latter was designed to produce a large-grained, peak-aged microstructure which could be adequately compared in terms of strength to as-rolled MAR209. Both the original material and the heat treated version were slow strain rate tested at a strain rate of 10⁻⁵ s⁻¹ in saturated ammonium chloride at 40°C.

As well as determining the type of fracture by using optical microscopy, the fractures were also prepared as sectioned micrographs polished to 1 µm finish for back-scattered electron imaging (BSI) and X-ray energy dispersive (EDS) analysis to determine whether there was a relationship between the microstructure and the fracture path. It was found useful to etch the grain boundaries slightly before SEM observation by the application of ethanolic ferric chloride.

Effect of Iron Content. A series of Cu-Ni-Al and Cu-Ni-Al-Mn-Nb alloys were produced in which the major aim was to produce differences in iron concentration. These were the alloys HMA130, MAR210, MAR211, MAR212, MAR213, MAR214 and MAR215 to which was added the Cu-Ni-Al alloy HMA120. The range of iron contents achieved was between 0.7% and 1.2% as shown in Table 1 (HMA120) and Table 2. Slow strain rate testing of the two Cu-Ni-Al alloys was carried out in 10% ammonium chloride at 82°C and the Cu-Ni-Al-Mn-Nb alloys were tested in saturated (30%) ammonium chloride at ambient temperature.

In order to establish fractography and to determine whether there was any visible relationship between stress corrosion susceptibility and microstructure, some fractured specimens were viewed in a Scanning Electron Microscope (SEM). Some fractures were also prepared as sectioned micrographs polished to 1 µm finish for back-scattered electron imaging (BSI) and X-ray energy dispersive (EDS) analysis to determine whether there was a relationship between the microstructure and the fracture path.

RESULTS

Hydrogen Embrittlement Testing

Results of slow strain rate tests carried out on a series of Cu-Ni-Al-Mn-Nb alloys with nickel content ranging between 19% and 25% are shown in Table 3. It can be seen that there is either no loss of ductility between samples tested under hydrogen charging conditions and those tested in air or the loss ductility is negligible. The mechanical test figures, coupled with the reported ductile fracture characteristics throughout, demonstrates that hydrogen embrittlement has not occurred.

Comparative stress corrosion resistance of different high strength copper-nickels

NACE TM-01-77 Static Loaded Tests. Results of the NACE TM-01-77 tests are given in Table 4. It can be seen that the two Cu-Ni-Al-Mn-Nb alloys sustained the 0.2% loading for the required 720 hours, whereas the Cu-Ni-Sn alloy failed after 180 hours. The fracture displayed by the Cu-Ni-Sn alloy was of a brittle intergranular nature.

NACE TM-0198-98 Slow Strain Rate Tensile Tests. Results of slow strain rate tests carried out on the three types of alloys, Cu-Ni-Sn, Cu-Ni-Al and Cu-Ni-Al-Mn-Nb in 10% ammonium chloride at 82°C are given in Table 5. Scanning electron micrographs of the fracture surfaces of the Cu-Ni-Sn and Cu-Ni-Al-Mn-Nb alloys respectively are shown in Figure 1 and Figure 2 after removing extraneous corrosion product with deaerated 50% hydrochloric acid (as per ASTM G1-81). The brittle intergranular nature of the fracture surface of the Cu-Ni-Sn alloy is evident, and the reduction of area ratio demonstrated by that alloy is low. The Cu-Ni-Al alloy displayed secondary cracking along the gauge length. The Cu-Ni-Al-Mn-Nb (Figure 2) exhibited ductile fractography, an absence of secondary cracking and a reduction of area ratio close to 1.00.

Investigation of the factors controlling stress corrosion susceptibility of Cu-Ni-Al and Cu-Ni-Al-Mn-Nb alloys

Degree of Ageing/ Heat treatment in the range 400°C-600°C. The results of the investigation of the effect of aging Cu-Ni-Al-Mn-Nb alloy (MAR208) on stress corrosion susceptibility¹⁰ are shown in Table 6. They show that the reduction of area ratio obtained by testing in the debilitating environment compared with that found by testing in air decreased as the aging heat treatment time increased. Also, the slow strain rate tensile sample which had been heat treated for 10 h at 480°C showed secondary cracking along the gauge length.

Grain Growth and Solutionising/ Heat treatment above 850°C. Results showing mechanical properties, grain size and slow strain rate reduction in area ratios for as-rolled MAR209 and the same alloy which had an applied heat treatment are given in Table 7. It can be seen that the grain size of the heat treated alloy is over three times larger than the as-rolled material.

Scanning Electron micrographs of polished and alcoholic ferric chloride etched sections of the two alloys are shown in Figure 3. The micrographs show the grain boundaries and the distribution of the micron-scale Ni-Nb-Fe-Si (ϵ -phase). It was found that the ϵ -phase is very much more associated with the grain boundaries in the case of the heat treated alloy (see Figure 3b). A higher magnification micrograph demonstrating this is shown in Figure 4.

Effect of Iron Content Results of slow rate tests of the two Cu-Ni-Al alloys with different iron concentrations (HMA120 and HMA130) are given in Table 8 and a relationship between iron content and the stress corrosion susceptibility is indicated. Scanning electron microscopy (SEM) was carried out on a polished micrograph of secondary cracks in HMA120, with one example being shown in Figure 5. EDS microanalysis was undertaken at the points on Figure 5 marked 1, 2, 3, 4, with points 2 and 3 being on the grain boundary crack. The spectra from points 2 and 3 showed distinct peaks indicating the presence of iron, whereas those of points 1

and 4 were less specific in this respect . Table 9 shows the iron content as approximately calculated from the spectra and there is a strong suggestion that iron is particularly associated with the grain boundary crack.

A relationship between alloy iron content and environmental sensitivity is also convincingly displayed in Figure 6, which plots the stress corrosion susceptibility (as measured by time to failure ratio) of the series of Cu-Ni-Al-Mn-Nb alloys with different iron concentrations. This clearly shows a tendency towards stress corrosion susceptibility as the iron content rises above 1%.

DISCUSSION

Hydrogen Embrittlement Testing

An interesting feature of the results, which show that Cu-Ni-Al-Mn-Nb alloys with nickel contents up to 25% are resistant to hydrogen embrittlement, is that it is widely reported that the Ni-Cu-Al alloy K-500 (UNS N05500) embrittles on exposure to hydrogen¹¹⁻¹³. As both these alloys precipitation harden through the formation of Ni₃Al, it would seem that, as the nickel content of this type of material rises from 25% to 65%, sensitivity to hydrogen embrittlement comes into effect. Work on measuring the hydrogen solubilities of the alloys has been carried out¹³ and this indicates that hydrogen is approximately twice as soluble in Ni-Cu-Al (-Mn-Nb) as it is in Cu-Ni-Al. However, this work also reported that the diffusion rates of hydrogen in the two materials was very similar at ambient temperature.

An explanation for the markedly different behavior of the two seemingly similar materials has been given by Pound,¹⁴ who carried out a mathematical analysis of the lattice diffusion and trapping of hydrogen in both Cu-Ni-Al-Mn-Nb and Ni-Cu-Al alloy (N05500). This analysis involved a model which was used to calculate the hydrogen ingress kinetics displayed by the two alloys under hydrogen charging conditions. Electrochemical experimental work was carried out to measure hydrogen entry and exit flux characteristics of the two materials. The result was that, with the supposition that the rate of hydrogen ingress is controlled by diffusion and the solution/metal interface causes a restriction on hydrogen entry, it was calculated that the irreversible hydrogen trapping ability of Cu-Ni-Al-Mn-Nb is approximately 40 times lower than that of Ni-Cu-Al. Thus hydrogen would be much more likely to be present within Ni-Cu-Al in a form which would facilitate the initiation of cracks.

Previous work on hydrogen embrittlement resistance of Cu-Ni-Al-Mn-Nb has been restricted to alloys containing less than 20% nickel, thus the present work demonstrates that the hydrogen embrittlement susceptibility (irreversible trapping ability) of this type of material continues to be low even when the nickel content rises to 25%.

Comparative stress corrosion resistance of different high strength copper-nickels

The brittle intergranular (IG) nature of the stress corrosion behavior of Cu-Ni-Sn displayed in both sulfide and ammonia environments is very reminiscent of the intergranular cracking observed in Cu-Zn alloys in ammonia.^{15,16} The current work failed to find evidence under high magnification of the presence of an intergranular film or observable crack arrest markings on the fracture surface of alloy MTA 150 after failure, and similar observations were made by Pickering and Byrne¹⁶ when they studied IG stress corrosion in Cu-Zn. The model they proposed was that a de-zincified layer adjacent to the grain boundary acted in a similar way to the presence of a brittle passive film in the film-rupture method of crack propagation¹⁵. Thus, the present work suggests that IG cracking of Cu-Ni-Sn occurs in an analogous manner to that of Cu-Zn, with segregation (or denudation) of tin in the grain boundary region giving rise to selective electrochemical dissolution along the grain boundary as a means of propagating the cracks. As shown by the SEM observations of the gauge length of a failed specimen (see Figure 1), the grain boundaries of Cu-Ni-Sn seem particularly prone to corrosive attack.

It has been found⁸ that, if high strength copper alloys are prone to stress corrosion in the presence of ammonium compounds, then they also display a decrease in mechanical properties in organic amines. These compounds are often present as curing agents in paints and adhesives or could be present in machining fluids, greases or cleaning agents. Thus, further investigations need to take place in order to determine whether Cu-Ni-Sn demonstrates environmental sensitivity under conditions of exposure to these substances.

In contrast to Cu-Ni-Sn, the Cu-Ni-Al-Mn-Nb alloys tested displayed resistance to stress corrosion cracking in both sulfide and ammonia environments. Alloy MAR220 was manufactured to be within a specific chemical composition range, as given in Table 10. Also, its manufacture was controlled in terms of maximizing aluminium in solution before hot working, ensuring that no hot working took place below a temperature of 800°C and ensuring that sufficient precipitation of Ni₃Al occurred during the cooling operation after hot-working. By controlling these operations, the material was able to achieve its required high mechanical properties whilst remaining in an under-aged condition. A high level of aluminium in solution was produced by heating the material slowly to the forging temperature and invoking a dwell period at a temperature of 850°C, where maximum dissolution of aluminium takes place. The reason why hot working is not sanctioned below 800°C is to prevent premature precipitation of Ni₃Al, which would reduce the intensity of the final hardening process which takes place during the air cool.

Investigation of the factors controlling stress corrosion susceptibility of Cu-Ni-Al and Cu-Ni-Al-Mn-Nb alloys

Degree of Aging/ Heat treatment in the range 400°C-600°C. It is apparent from the results of this investigation is that both ductility and stress corrosion susceptibility of Cu-Ni-Al-Mn-Nb are influenced by the degree of precipitation hardening. In the as-received condition, the alloy was evidently in a peak-aged state. Subsequent heat treatment produces additional precipitation, and this could either occur on existing Ni₃Al particles or take place at new nucleation sites. As the rate-controlling process for precipitate growth is diffusion, precipitates will tend to form most readily at grain boundaries, which would explain the onset of an observed embrittlement of the grain boundaries which takes place after a 10 hour heat treatment at 480°C.

The main conclusion of this exercise is that, when Cu-Ni-Al-Mn-Nb alloys are manufactured by a hot-working process, it would be beneficial, in terms of achieving resistance to stress corrosion, to produce it in an under-aged condition.

Grain Growth and Solutionising/ Heat treatment above 850°C. It is evident from the results produced in this work that the application of heat treatments which act to increase the grain size and which subsequently strengthen the material through precipitation hardening have a detrimental effect on stress corrosion resistance.

The SEM work strongly suggested that increasing the grain size caused a greater degree of association between the grain boundaries and the micron-scale ε-phase (Ni-Nb-Si-Fe-Cr) precipitates. This would have the effect of reducing the integrity of the grain boundary and could influence the grain boundary electrochemistry such that crack growth induced by selective phase attack would be increased. The ε-phase precipitates are necessary for producing grain refinement, as is demonstrated by the large grain size displayed by Cu-Ni-Al alloys⁹. However, it would be to some advantage to limit their volume fraction and produce a grain size which is small enough to avoid an association between these particles and the grain boundaries.

Regarding induction of stress corrosion sensitivity by heat treatments over 850°C, a microstructural investigation has been carried out on a hot-headed bolt in Cu-Ni-Al-Mn-Nb which failed after being exposed to an ammonium – based cleaning solution before being tensioned for application. Brittle intergranular failure was observed, and transmission electron microscopy carried out in a region near the failure found the occurrence of a duplex-type structure of Ni₃Al aging precipitates similar to that shown in Figure 7. The large precipitates were found to be very much associated with the grain boundaries, and the grain size was also found to be large. The history of this bolt was that it was hot-headed at a temperature of 1100°C, cooled and then given a further heat treatment for 2½

hours at 480°C. It was apparent from the microstructure that the cooling must have taken place unusually slowly and this part of the process has not been fully explained.

The major conclusion from this investigation was again that heat treatment of as-produced Cu-Ni-Al-Mn-Nb should not be undertaken if at all possible, particularly if it is at a temperature above 850°C.

Effect of Iron Content. The observation that the stress corrosion of the Cu-Ni-Al-Mn-Nb alloys tested in the current work is related to their iron content finds agreement with previous observations of this type. Work carried out on the stress corrosion cracking behavior of 90/10 copper nickels which contain iron in ammonia¹⁸ showed that resistance to SCC is produced by restricting the iron content to below 1% and retaining the iron in solution. It was found that, if the iron was above a level of 1% and out of solution, intergranular stress corrosion would result. Stress corrosion has also been found for 90/10 copper-nickel containing 1.4% Fe exposed to sodium sulfide in the concentration range 0.1M to 1M.¹⁹

In the case of the work by Popplewell,¹⁸ clear indications were given that grain boundary iron-containing precipitates could be formed after heat treatment at a temperature of 500°C. In the current work, it is less clear how iron could have such an influence, as the major grain boundary precipitates are Ni₃Al (which only contains a small concentration of iron) and the ε-phase (Ni-Nb-Si-Fe-Cr) precipitates.⁵ In the latter phase, iron makes up about 5% of the wt%, the principle elements present being nickel (~50%) and niobium (~35%). If the intergranular cracking is electrochemically controlled, as seems very likely from the fact that cathodic polarization produces stress corrosion resistance in Cu-Ni-Al-Mn-Nb,⁸ then it could be that the influence of iron on the grain boundary precipitate chemistry is on the active/passive behavior at the crack tip.¹⁵

The conclusion which can be made from this study is that it would be advantageous for stress corrosion resistance to limit the concentration of iron in Cu-Ni-Al-Mn-Nb alloys. As said previously, ε-phase grain refinement is necessary in the alloys, and iron is required to be present to effect precipitation of this phase. However, in the high strength Cu-Ni-Al-Mn-Nb alloys currently being produced for engineering applications, such as MAR220 in the present work, iron is being restricted to a maximum concentration of 0.85%.

The NACE TM-01-98-98 Slow strain Rate tensile Test

Throughout the investigations which have been reported in the current work the NACE TM-01-98-98 slow strain rate tensile test has proved very effective in discerning the degree of stress corrosion susceptibility of the different high strength copper-nickel alloys. As the manufacturing processes involved in producing stress corrosion-resistant high strength copper-nickels need to be carefully controlled, it would seem appropriate to employ a test such as the NACE TM-01-98-98 to prove each batch of product before release. Thus, the use of the NACE TM-01-98-98 slow strain rate tensile test is advocated as a production test method for very high strength copper alloys to verify resistance to stress corrosion cracking susceptibility.

CONCLUSIONS

Cu-Ni-Al-Mn-Nb alloys with nickel content up to 25wt% are resistant to hydrogen embrittlement.

Cu-Ni-Sn materials demonstrate susceptibility to stress corrosion in sulphide and ammonium environments whereas Cu-Ni-Al-Mn-Nb alloys with nickel content up to 25wt% are resistant to stress corrosion and stress corrosion in these environments.

A study of factors controlling stress corrosion susceptibility of Cu-Ni-Al and Cu-Ni-Al-Mn-Nb alloys shows the principal influences to be the degree of age hardening, the grain size and the iron content.

It is found necessary to control the production process of very high strength Cu-Ni-Al-Mn-Nb alloys such that high mechanical strengths are achieved with the material's possessing a fine grain size and being in an under-

aged condition. The alloy design should be such that a maximum volume of Ni₃Al precipitates are formed during air cooling after hot work and further heat treatment is not required.

The use of the NACE TM-01-98-98 slow strain rate tensile test is advocated as a production test method for very high strength copper alloys to verify resistance to stress corrosion cracking susceptibility.

REFERENCES

1. Copper Nickel Alloys- Properties and Applications, Publication by the Copper Development Association and the Nickel Development Institute, 1982
2. W. O. Alexander and D. J. Hanson, J Inst.Met., 61(1937),p. 83.
3. J. O. Ratka and M. N. Maligas, Paper No. 04298, Corrosion 2004, NACE, Houston
4. R. E Smallman, Modern Physical Metallurgy, 4th Edition, Butterworth-Heinemann Ltd, 1985, p.407
5. R. J. Grylls, C. D. S. Tuck, and M. H. Loretto, Intermetallics, 4 (1996), p. 567
6. R. J. Grylls, D. Phil. Thesis, University of Birmingham, UK, 1996
7. R J Grylls, C D S Tuck and M Loretto. Inst. Phys. Conf. Ser, No.147: Section 11 (1995) p. 459.
8. O Andersen, M W Joosten, J Murali and D E Milliams, "Evaluation of High Strength Cu-Ni-Mn-Al bolting used in oil and gas service", Corrosion/96 paper No. 78 (NACE International, Houston, Texas).
9. C. D. S. Tuck, N. Hort and B. L. Mordike. Paper No. 310, Corrosion /99, NACE, Houston
10. N. Hort, PhD Thesis, University of Clausthal, 2001
11. K. D. Eford, Materials Performance, April 1985, p. 37
12. D. M. Aylor, C. A. Bowles, R. L. Tregoning and M. A. Gaudett, International Workshop on Corrosion Control for Marine Structures and Pipelines, Galveston, 1999, American Bureau of Shipping, p. 279
13. C. D. S. Tuck, Zeng Xianghua, D. E. J. Talbot, Br.Corr.J 29, 1(1994):p. 70.
14. B. G. Pound, Corrosion 50, 4(1994):p. 301.
15. A. J. Bursle and E. N. Pugh, in Mechanisms of Environment-Sensitive Cracking of Materials, The Metals Society, London, 1977, p. 471
16. H. W. Pickering and P. J. Byrne, Corrosion, 29 (1973), p.325
17. R. J. Grylls, Unpublished work, University of Birmingham, UK, 1995
18. J. M. Popplewell, Corros. Sci, 13(1973):p. 593.
19. M. Islam, W. T. Riad, S. Al-Kharraz and S. Abo-Namour, Corrosion 47, 4(1991):p.260.

TABLE 1**COMPOSITION (wt%) AND MECHANICAL PROPERTIES OF THE ALLOYS USED IN THE HYDROGEN EMBRITTLEMENT, NACE TM-01-77-96 AND INITIAL NACE TM-01-98-98 TESTS**

Sample I.D	MAR216	MAR217	MAR218	MAR219	MTA150	HMA120	MAR220
Type of Alloy	Cu-Ni-Al-Mn-Nb	Cu-Ni-Al-Mn-Nb	Cu-Ni-Al-Mn-Nb	Cu-Ni-Al-Mn-Nb	Cu-Ni-Sn	Cu-Ni Al	Cu-Ni-Al-Mn-Nb
UNS/W Nr	C72420-	C72420-	C72420-	C72420-	C72900	W Nr	C72420-
Ni	18.91	19.10	24.17	25.09	14.9	13.96	19.25
Mn	4.37	4.37	5.32	5.21	-	0.30	4.24
Al	1.80	1.87	1.96	1.98	-	3.08	1.95
Fe	1.05	1.19	0.84	0.81	0.03	1.23	0.83
Cr	0.48	0.36	0.46	0.41	-	-	0.42
Nb	0.88	0.70	0.76	0.79	-	-	0.68
Sn	<0.01	<0.01	0.09	0.007	7.90		0.004
Cu	Bal	Bal	Bal	Bal	Bal	Bal	Bal
R _m (N/mm ²)	925	932	921	1006	917	953	943
R _{p,0.2} (N/mm ²)	713	702	709	781	765	820	707
A ₅ (%)	18	17.7	15	16	11	14	19
Hardness (HBN)	277	255	263	302	287	269	277
Impact Toughness CVN[-46°C] (J)	34, 32, 33	22, 23, 24	37, 39, 38	27, 26, 25	-	-	30, 32, 32

TABLE 2**COMPOSITION (wt%) AND MECHANICAL PROPERTIES OF THE ALLOYS USED IN THE INVESTIGATIVE STRESS CORROSION TESTS**

Sample ID	MAR208	MAR209	HMA130	MAR210	MAR211	MAR212	MAR213	MAR214	MAR215
Type of Alloy	Cu-Ni-Al-Mn-Nb	Cu-Ni-Al-Mn-Nb	Cu-Ni-Al	Cu-Ni-Al-Mn-Nb	Cu-Ni-Al-Mn-Nb	Cu-Ni-Al-Mn-Nb	Cu-Ni-Al-Mn-Nb	Cu-Ni-Al-Mn-Nb	Cu-Ni-Al-Mn-Nb
UNS/W Nr	C72420-type	C72420-type	W Nr 2.1504	C72420-type	C72420-type	C72420-type	C72420-type	C72420-type	C72420-type
Ni	18.93	1.89	14.4	19.21	19.10	17.45	19.43	17.8	18.96
Mn	4.52	4.32	0.23	4.20	4.60	3.85	4.49	4.47	4.20
Al	1.86	1.89	2.3	1.75	1.77	1.60	1.89	1.67	1.57
Fe	0.76	1.23	0.7	1.00	1.10	0.93	0.74	1.20	1.00
Cr	0.39	0.37	0.41	0.44	0.42	0.35	0.42	0.41	0.38
Nb	0.82	0.65	-	0.60	0.62	0.60	0.59	0.76	0.64
Sn	-	0.005	-	0.01	0.01	0.01	0.004	0.008	0.009
Cu	Bal	Bal	Bal	Bal	Bal	Bal	Bal	Bal	Bal
R _m (N/mm ²)	925	1002	927	974	972	938	93	959	929
R _{p,0.2} (N/mm ²)	730	791	790	715	703	727	723	775	711
A ₅ (%)	22.3	16	14.2	17	18	17	20.4	19.3	17
Hardness (HBN)	265	285	283	290	285	277	269	277	277
Impact Toughness CVN [-46°C] (J)	31, 32, 30	29, 29, 30	-	19, 20, 20	18, 19, 20	34, 32, 36	42, 40, 40	22, 22, 22	33, 32, 35

TABLE 3**RESULTS OF NACE TM-01-98-98 SLOW STRAIN RATE TESTS CARRIED OUT UNDER CATHODIC CHARGING AT -1V VS SCE IN ARTIFICIAL SEAWATER**

Sample ID	RA Ratio (%)	TF Ratio (%)	Observations
MAR216	1.06	1.09	No Corrosion No secondary cracking
MAR217	0.95	0.93	No Corrosion No secondary cracking
MAR218	1.25	1.03	No Corrosion No secondary cracking
MAR219	1.07	0.93	No Corrosion No secondary cracking

TABLE 4**RESULTS OF NACE TM-01-77-96 CONSTANT LOAD SULFIDE STRESS CORROSION TESTS CARRIED OUT AT A LOAD EQUIVALENT TO THE 0.2% PROOF STRESS**

Sample I.D	Duration of test compared to the required 720 hours (%)	Observations after test
MTA150	23%	Brittle intergranular failure
MAR216	100%	No cracking found
MAR217	100%	No cracking found
MAR218	100%	No cracking found
MAR219	100%	No cracking found

TABLE 5**RESULTS OF NACE TM-01-98-98 SLOW STRAIN RATE TESTS CARRIED OUT IN 10% AMMONIUM CHLORIDE AT 82°C**

Sample I.D	RA Ratio (%)	TF Ratio (%)	Observations
MTA150	0.62	0.53	Intergranular stress corrosion cracking.
HMA120	0.85	0.78	Evidence of secondary cracking along gauge length
MAR220	0.97	0.98	Ductile fracture. No secondary cracking.

TABLE 6**RESULTS OF SLOW STRAIN RATE TESTS CARRIED OUT AT THE UNIVERSITY OF CLAUSTRAL⁽¹⁰⁾ IN 20% SODIUM CHLORIDE AT 80°C ON SPECIMENS OF AS-ROLLED Cu-Ni-Al-Mn-Nb IN AN AS-RECEIVED CONDITION AND AFTER HEAT TREATMENT AT 480°C FOR VARIOUS TIMES**

Sample I.D	Heat treatment time (h)	Elongation in air (%)	RA Ratio (%)	Observations
MAR208	As received	20	1.0	Ductile fracture. No secondary cracking.
MAR208	480°C for 2½h	18	1.0	Ductile fracture. No secondary cracking.
MAR208	480°C for 5h	17	0.8	Ductile fracture. No secondary cracking.
MAR208	480°C for 10h	15	0.7	Ductile fracture. Evidence of secondary cracking along gauge length

TABLE 7

RESULTS OF SLOW STRAIN RATE TESTS CARRIED OUT IN SATURATED AMMONIUM CHLORIDE AT 20°C ON Cu-Ni-Al-Mn-Nb IN AS-RECEIVED CONDITION AND AFTER A HEAT TREATMENT AT 1000°C FOR 2 HOURS/AIR COOL TO 600°C/600°C FOR 2 HOURS/AIR COOL

Sample ID	Heat treatment	Grain Size (µm)	0.2% Proof Stress (N/mm ²)	Elongation in air (%)	Elong Ratio (%)	Observations
MAR209	480°C for 2½h/Air Cool	40	545	12.9	1.0	Ductile fracture - Small degree of secondary cracking along gauge length
MAR209	1000°C for 2h/Air cool to 600°C/600°C for 2h/Air cool	150	568	10.9	0.8	Brittle fracture. High degree of secondary cracking along gauge length.

TABLE 8

RESULTS OF SLOW STRAIN RATE TESTS CARRIED OUT IN 10% AMMONIUM CHLORIDE AT 82°C ON TWO Cu-Ni-Al ALLOYS WITH DIFFERENT IRON CONTENTS PRODUCED AS 25mm DIAMETER ROLLED BAR

Sample I.D	Iron Content (wt%)	RA Ratio (%)	TF Ratio (%)
HMA120	1.23	0.85	0.78
HMA130	0.70	1.20	1.00

TABLE 9

RESULTS SHOWING X-RAY ENERGY DISPERSIVE SPECTRAL ANALYSIS CALCULATION OF IRON CONCENTRATION AT THE SPOTS 1, 2, 3 AND 4 OF THE SCANNING ELECTRON MICROGRAPH SHOWN IN FIGURE 5

Point Number	Calculated iron concentration (wt%)
1	0.9
2	1.1
3	1.3
4	0.9

TABLE 10

COMPOSITION OF Cu-Ni-Al-Mn-Nb ALLOY MAR220 OPTIMIZED FOR HIGH MECHANICAL PROPERTIES AND RESISTANCE TO STRESS CORROSION

	Composition, %
Aluminium	1.60 - 2.20
Iron	0.65 – 0.85
Nickel	18.00 - 25.00
Manganese	4.00 – 5.60
Chromium	0.36 – 0.48
Niobium	0.55 – 0.90
Total impurities	0.15 Max
Copper	REM

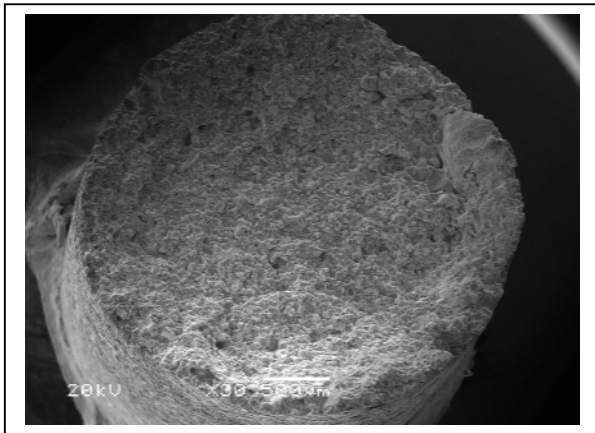


FIGURE 1. Scanning electron micrograph of the fracture face and adjacent gauge length surface of alloy Cu-Ni-Sn alloy (MTA150) after slow strain rate testing in an environment of 10% NH₄Cl at 82°C. Magnification x17.

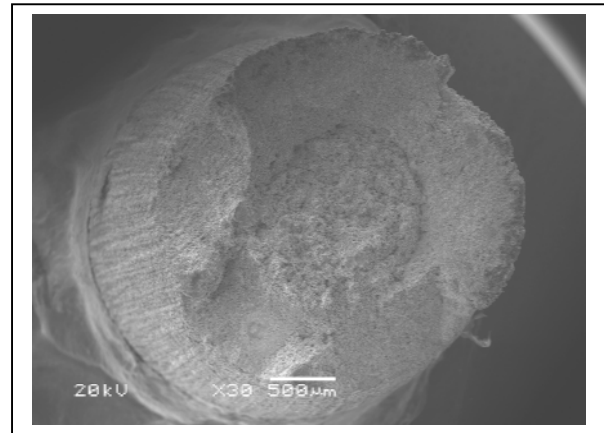


FIGURE 2. Scanning electron micrograph of the fracture face and adjacent gauge length surface of alloy Cu-Ni-Al-Mn-Nb alloy (MAR220) after slow strain rate testing in an environment of 10% NH₄Cl at 82°C. Magnification x17.

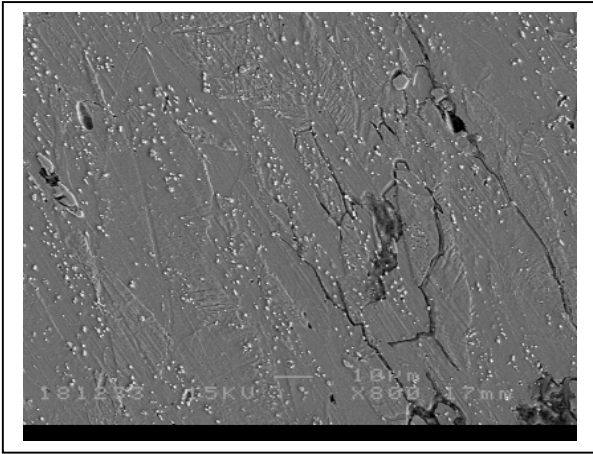


FIGURE 3(a). Scanning electron micrograph of a polished and etched metallographic specimen of as-received MAR209 after slow strain rate testing in an environment of 30% NH₄Cl at 20°C. Magnification x500.

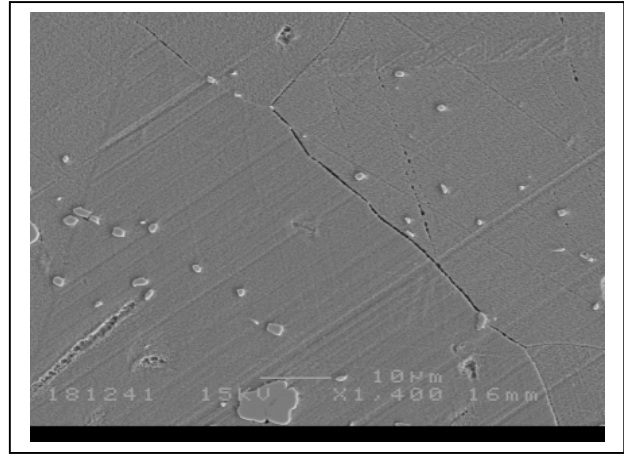


FIGURE 3(b). Scanning electron micrograph of a polished and etched metallographic specimen of MAR209 which has received a heat treatment of 1000°C (2h) followed by 600°C (2h) after slow strain rate testing in an environment of 30% NH₄Cl at 20°C. Magnification x900.

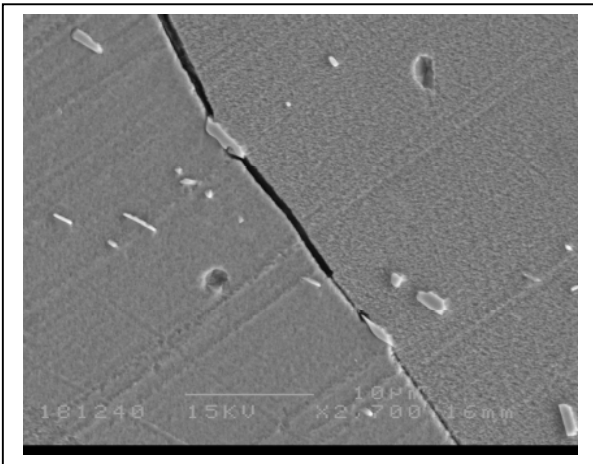


FIGURE 4. Higher magnification scanning electron micrograph of the metallographic sample of Figure 3(b) showing the relationship between the micron-scale phases and the grain boundaries. Magnification x1550.

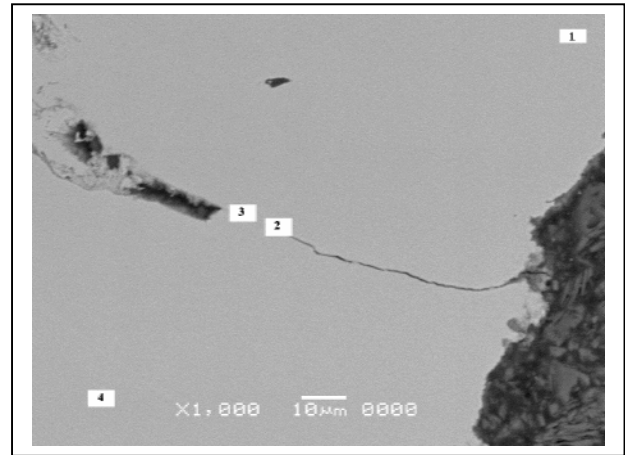


FIGURE 5. Scanning electron micrograph of a polished metallographic specimen of HMA120 which has been slow strain rate tensile tested in 10% NH₄Cl at 82°C. Points 1, 2, 3 and 4 denote spot which were chemically analysed by EDS. Magnification x550

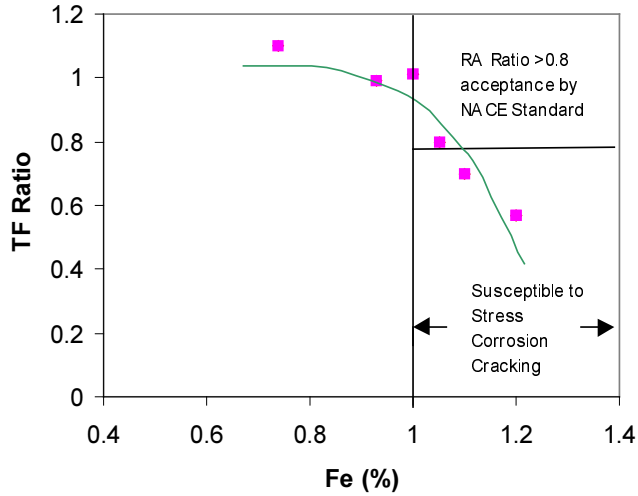
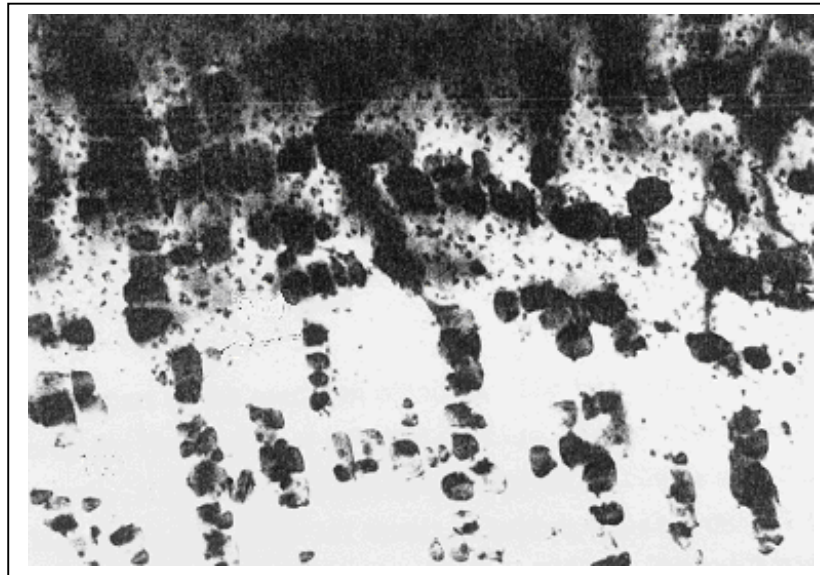


FIGURE 6. A graph showing the relationship between iron content of several Cu-Ni-Al-Mn-Nb alloys with their stress corrosion susceptibility, as measured by the time to failure (TF) ratio after slow strain rate testing in 30% ammonium chloride at 20°C



500nm

FIGURE 7. Transmission electron micrograph⁶ showing a grossly over-aged microstructure in a Cu-Ni-Al-Mn-Nb alloy created through the application of a heat treatment consisting of 900°C for 2h, ice brine quench followed by 715°C for 500 hours with air cooling. Magnification x36,000.